methyl ethylenediamine (0.14 mL, 0.91 mmol) was then added, and the reaction mixture was reduced to give orange microcrystals quantitatively. The analytical sample was prepared by cooling a saturated dichloromethane solution: ^{1}H NMR (C_6D_6) δ 12.20 (t, 1, J_{HH} = 7, C*H*Et), 4.57 (m, 2, CHCH_2Me), 2.27 (br s, 12, NMe_2), 2.01 (s, 4, $Me_2NCH_2CH_2NMe_2$), 1.43 (s, 6, OCMe(CF_3)$_2$), 1.16 (s, 9, CMe_3), 1.02 (t, 3, J_{HH} = 8, CHCH$_2$$Me$); ^{13}C NMR ($C_6D_6$) δ 287.12 (*C*CMe$_3$), 273.29 (J_{CH} = 125, *C*HEt), 125.91 (J_{CF} = 290, *C*F$_3$), 81.04 (*OC*Me(CF_3)$_2$), 59.11 (J_{CH} = 135, $Me_2NCH_2CH_2NMe_2$), 54.0 (*C*Me$_3$), 48.99 (J_{CH} = 125, *C*H$_2$Me), 30.81 (NMe_2), 28.62 (CH$_2$$Me$), 21.06 (C$Me_3$), 17.34 (OC$Me$($CF_3$)$_2$). Anal. Calcd for $C_{24}H_{41}F_{12}N_2O_2Re$: C, 35.86; H, 5.14; N, 3.48. Found: C, 35.93; H, 5.04; N, 3.87.

Metathesis of *cis*-2-Pentene by Re(C-*t*-Bu)(CH-*t*-Bu)(OR_{F6})$_2$. *cis*-2-Pentene (0.55 mL, 5 mmol) was added to a solution of *syn*-Re(C-*t*-Bu)(CH-*t*-Bu)(OR_{F6})$_2$ (0.05 mmol) in 5.0 mL of benzene in a septum-capped vial. Aliquots were periodically withdrawn with a syringe and quenched by passage through activated alumina, a procedure that a separate experiment showed to result in complete loss of metathesis activity. The concentrations of the 2-butenes, 2-pentenes, and 3-hexenes were determined by gas chromatography. After 2.5 h at room temperature, equilibrium was achieved. Upon addition of another 100 equiv of *cis*-2-pentene to the remaining catalyst mixture, equilibrium was reestablished in 30 min.

Metathesis of Methyl Oleate by Re(C-*t*-Bu)(CH-*t*-Bu)(OR_{F6})$_2$. To a solution of *syn*-Re(C-*t*-Bu)(CH-*t*-Bu)(OR_{F6})$_2$ (0.05 mmol) in 5.0 mL of methylene chloride was added an internal standard of mesitylene (35 μL, 0.25 mmol) and then 50 equiv of methyl oleate (0.85 mL, 2.52 mmol). The solution was stirred vigorously, and aliquots were periodically withdrawn and quenched by passage through activated alumina. The concentrations of the metathesis products were then determined by gas chromatography. Equilibrium was achieved within 12 h at room temperature. This catalyst solution was then allowed to remain undisturbed for an additional 24 h, and an additional 50 equiv of methyl oleate was added to the remaining catalyst mixture. Equilibrium was reestablished within 7.5 h at room temperature.

Increased Rate of Methyl Oleate Metathesis by Addition of *cis*-3-Hexene to Re(C-*t*-Bu)(CH-*t*-Bu)(OR_{F6})$_2$. To a solution of *syn*-Re(C-*t*-Bu)(CH-*t*-Bu)(OR_{F6})$_2$ (0.038 mmol) in 2.00 mL of methylene chloride was added 10 equiv of *cis*-3-hexene (47 μL, 0.38 mmol). The solution was then stirred for 7 h in order to prepare Re(C-*t*-Bu)(CHEt)(OR_{F6})$_2$ in situ, and an additional 3.0 mL of methylene chloride and an internal standard of 1-phenyloctane (84 μL, 0.38 mmol) were then added. Methyl oleate (50 equiv) was then added. Equilibrium was achieved within 180 min at room temperature. After an additional 12.5 h at room temperature, an additional 100 equiv of methyl oleate was added to the catalyst mixture. Equilibrium was reestablished within 6 h.

Acknowledgment. R.R.S. thanks the National Science Foundation (Grant CHE 91-22827) for research support, R.T. thanks Catalytica Associates, Inc. for a graduate fellowship, and G.A.V. thanks the National Institutes of Health for a postdoctoral fellowship. We thank Mike Vale for solving the structure of the Re(CHOEt) complex and Catalytica Associates, Inc. for a gift of methyl 9-decenoate.

Supplementary Material Available: ORTEP drawing, fully labeled drawing, and tables of final positional parameters and final thermal parameters for *syn*-Re(C-*t*-Bu)(CHOEt)(OR_{F6})$_2$(THF)$_2$ and *anti*-Re(C-*t*-Bu)(CHFc)(OR_{F6})$_2$ (12 pages); listings of final observed and calculated structure factors for *syn*-Re(C-*t*-Bu)(CHOEt)(OR_{F6})$_2$(THF)$_2$ and *anti*-Re(C-*t*-Bu)(CHFc)(OR_{F6})$_2$ (74 pages). Ordering information is given on any current masthead page.

Exploiting Laser Based Methods for Low-Temperature Solid-State Synthesis: Growth of a Series of Metastable $(Sr_{1-x}M_x)_{1-\delta}CuO_2$ Materials

Chunming Niu and Charles M. Lieber*

Contribution from the Department of Chemistry and Division of Applied Sciences, Harvard University, Cambridge, Massachusetts 02138. *Received June 30, 1992*

Abstract: Pulsed laser deposition (PLD) has been used to prepare a series of $(Sr_{1-x}Ca_x)_{1-\delta}CuO_2$ thin film materials on ⟨100⟩ $SrTiO_3$ and ⟨100⟩ MgO at low temperatures. X-ray diffraction (XRD), electron diffraction (ED), and ion-channeling studies have shown that all of the $(Sr_{1-x}Ca_x)_{1-\delta}CuO_2$ materials (x = 0–1; δ = 0.1) grown on ⟨100⟩ $SrTiO_3$ at 500 °C have a layered, tetragonal structure with the c-axis oriented perpendicular to the substrate surface. In contrast, the target materials prepared by conventional high-temperature techniques have an orthorhombic structure (x = 0, δ = 0) or consist of multiple phases (x = 0, δ = 0.1; x > 0, δ = 0, 0.1). Rutherford backscattering studies have shown that the composition of the materials prepared by PLD are the same as the starting target stoichiometry, even when the targets contain multiple phases. The dependence of the product structure on growth temperature and substrate lattice constant were also determined. $SrCuO_2$ materials grown at 500, 600, and 700 °C exhibit a decreasing ratio of tetragonal/orthorhombic phase as the temperature increases. These results show that low-temperature growth traps the layered, tetragonal phase. Comparison of the $SrCuO_2$ structures obtained on ⟨100⟩ $SrTiO_3$ and ⟨100⟩ MgO substrates have also shown that product–substrate lattice matching is important in stabilizing the tetragonal phase and in orienting the crystallographic growth direction. In addition, the physical properties of these new materials have been characterized by electrical and magnetic measurements. The stoichiometric $(Sr_{1-x}Ca_x)_{1-\delta}CuO_2$ materials were found to be insulators. However, the nonstoichiometric $(Sr_{1-x}Ca_x)_{1-\delta}CuO_2$ materials exhibited systematic increases in conductivity with decreasing x. Furthermore, the x = 0 material, $Sr_{0.9}CuO_2$, showed a transition to a zero resistance state with an onset of ≈20 K. The implications of these studies to copper oxide superconductors are discussed.

Introduction

The synthesis of materials by conventional ceramic methods requires high reaction temperatures in order to facilitate diffusion and reaction in the solid state.[1-3] As a consequence, the products derived from conventional solid-state methodologies are limited typically to the ones thermodynamically stable at high temperature. In the past most solid-state synthetic studies have focused on high-temperature reaction chemistry; however, there is now a considerable and rapidly growing interest in the development

(1) (a) Corbett, J. D. In *Solid State Chemistry: Techniques*, Cheetham, A. K., Day, P., Eds.; Oxford University Press: New York, 1987; p 1. (b) West, A. R. *Solid State Chemistry and Its Applications*; John Wiley and Sons: New York, 1984.

(2) (a) Hagenmuller, P. *Preparative Methods in Solid State Chemistry*; Academic Press: New York, 1972. (b) Rao, C. N. R.; Gopalakrishnan, J. *New Directions in Solid State Chemistry*; Cambridge University Press: New York, 1986.

(3) DiSalvo, F. J. *Science* **1990**, *247*, 649.

0002-7863/93/1515-137$04.00/0

of low-temperature approaches to materials synthesis.[3-12] Controlled low-temperature synthesis is a particularly intriguing goal since it offers the possibility of obtaining new phases and materials which may exhibit novel physical properties.

Several different approaches to low-temperature solid-state synthesis have been reported, including (i) solution-phase reaction and crystallization from low-temperature fluxes;[4,5] (ii) decomposition of molecular precursors;[6-8] and (iii) laser ablation and deposition.[9-12] Polychalcogenide reactive fluxes have been used by several groups to prepare new metal chalcogenide clusters and solids at temperatures ≥200 °C.[4,5] These results indicate that the reactive flux method is a promising technique for low-temperature synthesis; however, it is not yet possible to predict a priori the products from these flux reactions. A second synthetic approach that has attracted considerable attention involves decomposing molecular precursors in the solid state.[6-8] In principle, this method minimizes the problem of diffusion in the solid state, although high temperatures are often needed to obtain crystalline products. The chemical precursor approach has been used to prepare metal chalcogenides materials,[7] an unusual phase of tantalum nitride,[8] and other solids.[6] In addition, chemical precursors are widely used industrially for vapor phase deposition of thin films.[13]

A significantly different approach to the low-temperature synthesis of materials is pulsed laser ablation and deposition (PLD). PLD is a well-established technique for the growth of highly crystalline thin films of known materials.[9] Experimentally, this methodology involves ablation of a target using a high-energy pulsed laser and subsequent deposition of the ablation material onto a substrate to yield a thin film product. In the past PLD has been used to prepare high-quality films of a variety of known solids, such as ferro- and piezoelectric materials,[14] semiconductor superlattices,[15] and copper oxide superconductors.[16,17] There are, however, a number of features of the ablation and deposition processes which are ideal for the synthesis of new materials. Two of the most important features are (i) congruent target evaporation during rapid laser heating and (ii) crystalline product growth at temperatures significantly lower than conventional solid-state reactions. Few studies have, however, utilized these features for the synthesis of new materials.[10-12,18] Herein, we report investigations of the synthesis of a series of layered $(Sr_{1-x}Ca_x)_{1-\delta}CuO_2$ materials by PLD. In a preliminary account we prepared the $x = \delta = 0$ material.[10] The present studies demonstrate the systematic synthesis of a wide range of new materials that are inaccessible by conventional high-temperature preparative methods. Mechanistic studies have shown that the layered $(Sr_{1-x}Ca_x)_{1-\delta}CuO_2$ products are formed by trapping the product at the low-temperature growth conditions accessible in the PLD experiment. In addition, the new materials prepared in these investigations exhibit interesting electrical properties and may serve as excellent systems in which to probe high-temperature superconductivity.

Table I. PLD Synthetic Conditions

substrate	⟨100⟩ $SrTiO_3$ or ⟨100⟩ MgO
substrate temperature	500–700 °C
substrate-target distance	3.5–4 cm
O_2 partial pressure	10 mTorr
irradiation wavelength	248 nm
power density	1–2 J/cm²
pulse repetition rate	5 Hz

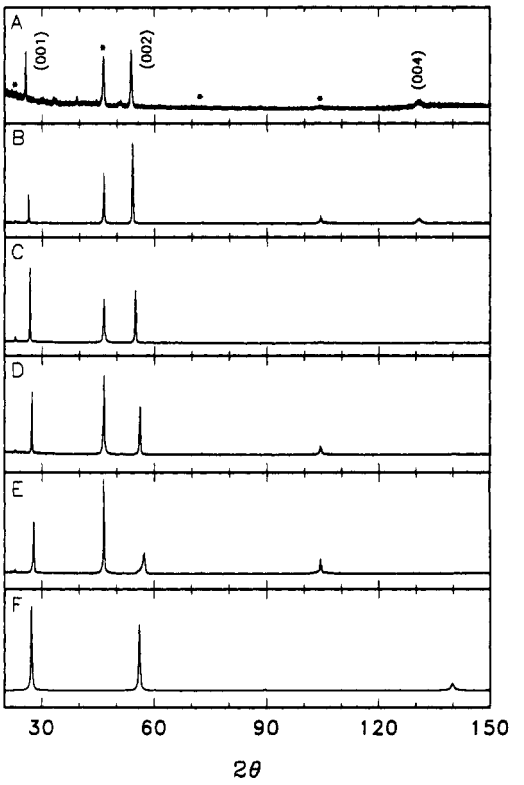

Figure 1. XRD diffraction patterns recorded on (A) $SrCuO_2$, (B) $Sr_{0.7}Ca_{0.3}CuO_2$, (C) $Sr_{0.5}Ca_{0.5}CuO_2$, (D) $Sr_{0.3}Ca_{0.7}CuO_2$, and (E) $CaCuO_2$ samples prepared by PLD at 500 °C on ⟨100⟩ $SrTiO_3$. A simulation of the diffraction pattern for tetragonal $SrCuO_2$ with the c-axis oriented perpendicular to the substrate surface is shown in (F). The (100), (200), (300), and (400) $SrTiO_3$ substrate peaks occurring at 2θ = 22.77, 46.50, 72.56, and 104.17, respectively, are marked with asterisks (*).

Experimental Methods

Target Preparation. $(Sr_{1-x}Ca_x)_{1-\delta}CuO_2$ targets were prepared by conventional high temperature synthesis. Briefly, stoichiometric amounts of $SrCO_3$ (99.999%, Johnson Matthey), $CaCO_3$ (99.999%, Johnson

(4) (a) Sunshine, S. A.; Kang, D.; Ibers, J. A. *J. Am. Chem. Soc.* **1987**, *109*, 6202. (b) Keane, P. M.; Lu, Y.-J.; Ibers, J. A. *Acc. Chem. Res.* **1991**, *24*, 223.

(5) (a) Kanatzidis, M. G.; Huang, S.-P. *J. Am. Chem. Soc.* **1989**, *111*, 760. (b) Kanatzidis, M. G.; Park, Y. *J. Am. Chem. Soc.* **1989**, *111*, 3767. (c) Kanatzidis, M. G. *Chem. Mater.* **1990**, *2*, 353.

(6) *Transformation of Organometallics into Common and Exotic Materials: Design and Activation*; Laine, R. M., Ed.; Nato Advanced Science Institute Series; Martinus Nijhoff: Dordrecht, 1988.

(7) (a) Steigerwald, M. L.; Rice, C. E. *J. Am. Chem. Soc.* **1988**, *110*, 4228. (b) Steigerwald, M. L. *Chem. Mater.* **1989**, *1*, 52. (c) Brennan, J. G.; Siegrist, T.; Stuczynski, S. M.; Steigerwald, M. L. *J. Am. Chem. Soc.* **1990**, *112*, 9233.

(8) (a) Banaszak Holl, M. M.; Kersting, M.; Pendley, B. D.; Wolczanski, P. T. *Inorg. Chem.* **1990**, *29*, 1518. (b) Banaszak Holl, M. M.; Wolczanski, P. T.; Van Duyne, G. D. *J. Am. Chem. Soc.* **1990**, *112*, 7989.

(9) (a) Cheung, J. T.; Sankur, H. *CRC Crit. Rev. Solid State Mater. Sci.* **1988**, *15*, 63. (b) Olander, D. R. *High Temp. Sci.* **1990**, *27*, 411. (c) Paine, D. C.; Bravman, J. C. *Laser Ablation for Materials Synthesis*; Materials Research Society: Pittsburgh, PA, 1990.

(10) Niu, C.; Lieber, C. M. *J. Am. Chem. Soc.* **1992**, *114*, 3570.

(11) (a) Norton, D. P.; Lowndes, D. H.; Sales, B. C.; Budai, J. D.; Chakoumakos, B. C.; Kerchner, H. R. *Phys. Rev. Lett.* **1991**, *66*, 1537. (b) Fincher, C. R.; Blanchet, G. B. *Phys. Rev. Lett.* **1991**, *67*, 2902.

(12) (a) Tabata, H.; Murata, O.; Kawai, T.; Kawai, S. *Appl. Phys. Lett.* **1990**, *56*, 1576. (b) Li, X.; Kanai, M.; Kawai, T.; Kawai, S. *Jpn. J. Appl. Phys.* **1992**, *31*, L217.

(13) Tietjen, J. J. *Ann. Rev. Mater. Sci.* **1973**, *3*, 317.

(14) (a) Otsubo, S.; Maeda, T.; Minamikawa, T.; Yonezawa, Y.; Morimoto, A.; Shimizu, T. *Jpn. J. Appl. Phys.* **1989**, *26*, L133. (b) Chrisey, D. B.; Horwitz, J. S.; Grabowski, K. S. *Mat. Res. Soc. Symp. Proc.* **1990**, *191*, 25.

(15) (a) Cheung, J. T.; Niizawa, G.; Moyle, J.; Ong, N. P.; Paine, B. M.; Vreeland, T., Jr. *J. Vac. Sci. Tech. A* **1986**, *4*, 2086. (b) Cheung, J. T.; Madden, J. *J. Vac. Sci. Tech. B* **1987**, *5*, 705.

(16) (a) Xi, X. X.; Venkatesan, T.; Li, Q.; Wu, X. D.; Inam, A.; Chang, C. C.; Ramesh, R.; Hwang, D. M.; Ravi, T. S.; Findikoglu, A.; Hemmick, D.; Etemad, S.; Martinez, J. A.; Wilkens, B. *IEEE Trans. Magn.* **1991**, *27*, 2. (b) Koren, G.; Gupta, A.; Baseman, R. J.; Lutwyche, M. I.; Laibowitz, R. B. *Appl. Phys. Lett.* **1989**, *55*, 2450. (c) Izumi, H.; Ohata, K.; Sawada, T.; Morishita, T.; Tanaka, S. *Appl. Phys. Lett.* **1991**, *59*, 597. (d) Gupta, A.; Braren, B.; Casey, K. G.; Hussey, B. W.; Kelly, R. *App. Phys. Lett.* **1991**, *59*, 1302.

(17) (a) Triscone, J.-M.; Fischer, O.; Brunner, O.; Antognazza, L.; Kent, A. D.; Karkut, M. G. *Phys. Rev. Lett.* **1990**, *64*, 804. (b) Lowndes, D. H.; Norton, D. P.; Budai, J. D. *Phys. Rev. Lett.* **1990**, *65*, 1160. (c) Matsumoto, T.; Kawai, T.; Kitahama, K.; Kawai, S. *Appl. Phys. Lett.* **1991**, *58*, 2039. (d) Kawai, T.; Egami, Y.; Tabata, H.; Kawai, S. *Nature* **1991**, *349*, 17.

(18) Kawai, T.; Egami, Y.; Tabata, H.; Kawai, S. *Nature* **1991**, *349*, 200.

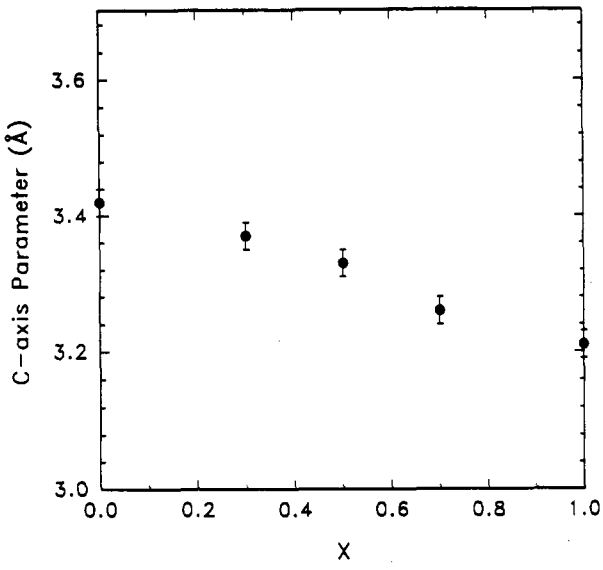

Figure 2. Dependence of the *c*-axis lattice parameter as a function of x in $Sr_{1-x}Ca_xCuO_2$ materials grown by PLD at 500 °C.

Matthey), and CuO (99.999%, Johnson Matthey) were ground, reacted in air at 800 °C for 12 h, reground, and heated at 900 °C for 24 h. The resulting polycrystalline material was pressed (3000 l.c. PSI) into a 20-mm o.d. pellet and sintered at 950 °C. This preparative route generally yields products that are multiphase; the $x = \delta = 0$ material ($SrCuO_2$) is, however, single phase with an orthorhombic structure.[19]

Film Deposition. The PLD experiments were carried out in a stainless steel vacuum chamber that is evacuated with a turbomolecular pump.[10] The target was mounted inside the chamber on a feedthrough that was rotated during ablation. The ablation was carried out using a KrF excimer laser (Lambda Physik, 105) at a power density of 1–2 J/cm^2 and a repetition rate of 5 Hz. The ablated material was directed onto a heated substrate diametrically opposed to the irradiated target; the substrate was located 3.5–4 cm from the target. Both ⟨100⟩ $SrTiO_3$ and ⟨100⟩ MgO single crystals (MarkeTech International) were used as substrates.

Film Characterization. X-ray diffraction (XRD) patterns (θ–2θ) were measured using Cu $K\alpha_1$ radiation; data were collected from 6–150° at a scan rate of 1°/min. Electron diffraction (ED) measurements were made perpendicular to the substrate surface using a Philips EM420T transmission electron microscope; the beam energy was 120 keV. Samples for ED were prepared using standard methods.[20] Briefly, the film/substrate was ground mechanically, dimpled, and then thinned to electron transparency by Argon-ion milling at 77 K. Rutherford backscattering (RBS) measurements were made using 2.0 MeV helium ions (General Ionics, Model 4117) in both aligned and random geometries. Simulations were carried out using standard software.[21] Resistivity measurements were made using a computer controlled four-probe apparatus, and magnetic data were collected using a commercial superconducting quantum interference device (SQUID) based magnetometer (MPMS2, Quantum Design).

Results

Synthesis and Characterization of $Sr_{1-x}Ca_xCuO_2$. Typical PLD preparation conditions used in these studies are summarized in Table I. Ablation of $Sr_{1-x}Ca_xCuO_2$ (x = 0, 0.3, 0.5, 0.7, and 1) targets and deposition on ⟨100⟩ $SrTiO_3$ substrates at 500 °C leads to crystalline materials that are structurally distinct from the target materials. XRD scans of the new materials prepared by PLD are shown in Figure 1. All of these thin film materials can be indexed as a tetragonal $MCuO_2$ infinite layer phase with the *c*-axis oriented perpendicular to the substrate surface. A simulation of the XRD pattern expected for this orientated, tetragonal structure is shown in Figure 1F and is in excellent agreement with the experimental results. In contrast, XRD scans of the targets can only be indexed to the known orthorhombic phase of $SrCuO_2$ (x = 0) or mixtures of this orthohombic phase and other impurity phases (x = 0.3, 0.5, 0.7, and 1). We also find that the *c*-axis parameter calculated from the XRD data systematically decreases in the new materials prepared from targets with increasing x (Figure 2).

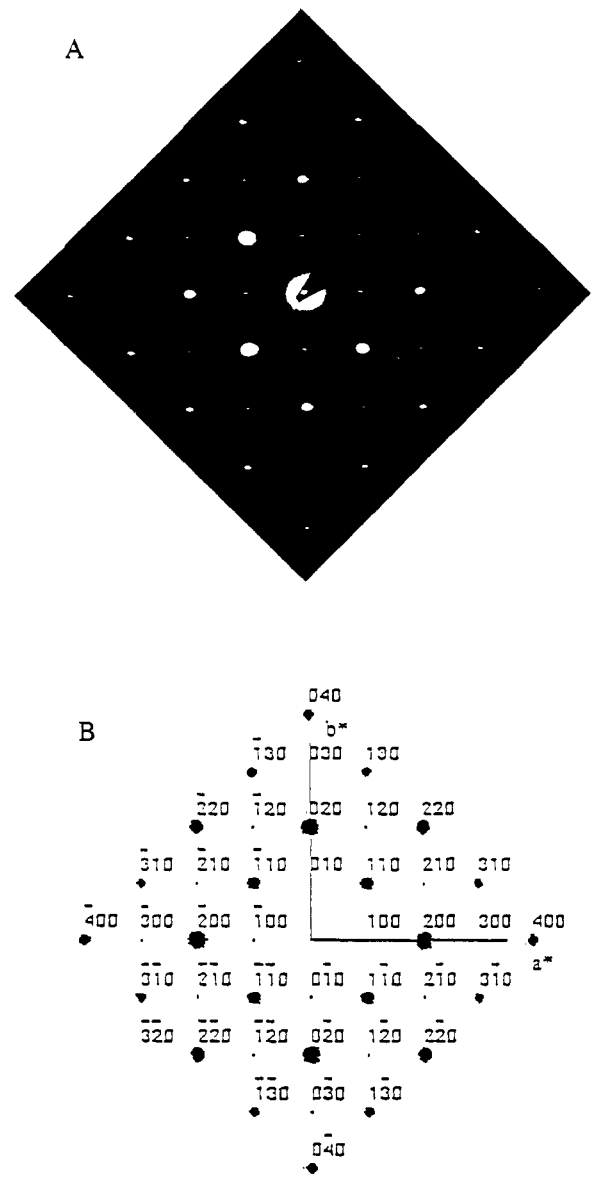

Figure 3. (A) ED pattern recorded along the (001) zone axis of a $Sr_{0.7}Ca_{0.3}CuO_2$ sample prepared at 500 °C on ⟨100⟩ $SrTiO_3$. (B) Simulation of the ED pattern for tetragonal $Sr_{0.7}Ca_{0.3}CuO_2$.

ED investigations of the new thin film $Sr_{1-x}Ca_xCuO_2$ materials were also carried out. A typical ED pattern obtained along the [001] zone axis on a $Sr_{0.7}Ca_{0.3}CuO_2$ thin film sample is shown in Figure 3A. This pattern can be readily indexed as the layered tetragonal phase. A simulation of the expected diffraction pattern along the [001] zone axis exhibits excellent agreement with the experimental data (Figure 3B). The electron diffraction results are thus consistent with the structural assignment from the XRD.

The composition of the $Sr_{1-x}Ca_xCuO_2$ materials prepared by PLD were determined by RBS. Typical results are shown in Figure 4. These data show that the metal stoichiometry of the films is the same as the average composition of the targets within the 5% uncertainty of the RBS measurement and analysis procedures. For example, ceramic $Sr_{1-x}Ca_xCuO_2$ targets with x = 0, 0.3, 0.86, and 1 gave films with Sr/Ca/Cu stoichiometries of 1:0:1.05, 0.71:0.29:1.02, 0.15:0.83:1.01, and 0:0.97:1.04, respectively. In addition, the ion channeling yield determined for $Sr_{0.7}Ca_{0.3}CuO_2$, which has a good lattice match with the ⟨100⟩

(19) Teske, V. C. L.; Muller-Buschbaum, H. *Anorg. Allg. Chem.* **1970**, *379*, 234.

(20) Thomas, G.; Goringe, M. J. *Transmission Electron Microscopy of Materials*; Wiley-Interscience: New York, 1979.

(21) The RBS data analysis was carried out using the program *RUMP* from the Department of Materials Science and Engineering, Cornell University.

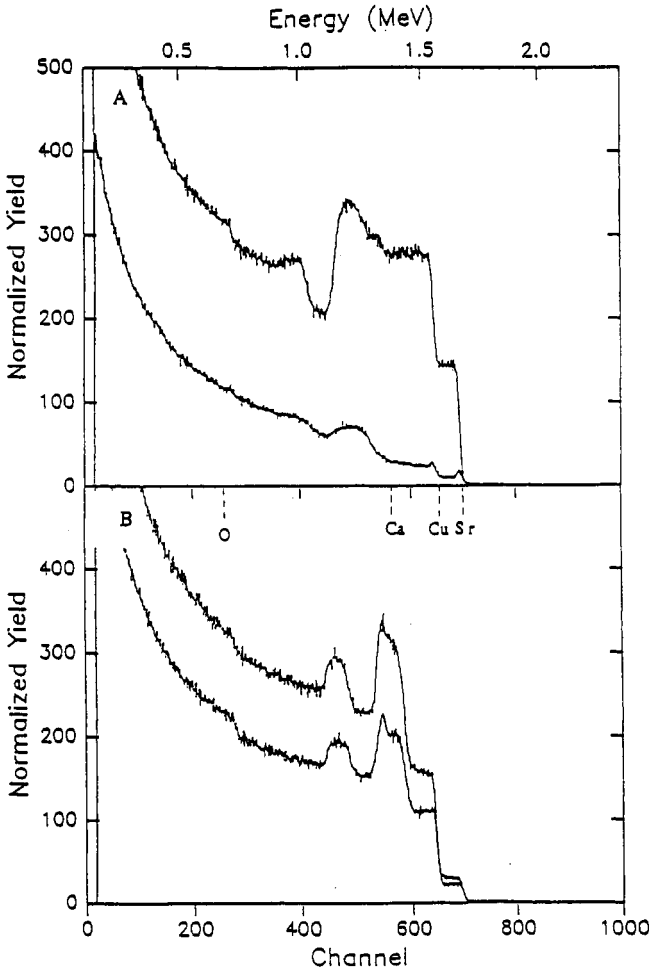

Figure 4. RBS results obtained on (A) $Sr_{0.7}Ca_{0.3}CuO_2$ and (B) $Sr_{0.14}Ca_{0.86}CuO_2$ materials prepared at 500 °C on ⟨100⟩ $SrTiO_3$. The upper traces in (A) and (B) correspond to the back-scattered yield for random sample orientation. The lower traces in (A) and (B) represent the channeling yield with the ion beam aligned along the *c*-axis of the materials.

$SrTiO_3$ substrate, was only 6%. This yield is comparable to the 3–6% channeling yield expected for a true single crystal sample. These data thus show that our product is a highly-oriented, single-crystal-like material that does not contain intergrowths.

Growth Mechanism. The effects of growth temperature and substrate lattice constant were investigated to determine factors important for the preparation of the layered, tetragonal phase. The role of temperature was studied for $SrCuO_2$ ($x = 0$) growth on ⟨100⟩ $SrTiO_3$ substrates. The XRD patterns obtained from materials grown by PLD at 500, 600, and 700 °C are shown in Figure 5. Analyses of the XRD patterns recorded from $SrCuO_2$ films grown at 500 °C show almost exclusive formation of the layered, tetragonal phase oriented with the *c*-axis perpendicular to the substrate surface. Small impurity peaks are also observed at $2\theta = 34.4°$ and 40.3°; these peaks can be indexed as the (111) and (061) peaks of the orthorhombic phase. Comparison of the peak intensities for the tetragonal phase versus the orthorhombic phase show that >90% of the $SrCuO_2$ material grown at 500 °C corresponds to the layered, tetragonal phase. The XRD patterns recorded on $SrCuO_2$ thin films grown at $T > 500$ °C exhibit significant changes. $SrCuO_2$ grown at 600 °C consists of ≈40% tetragonal phase and 60% orthorhombic phase (Figure 5B). Diffraction patterns recorded on material grown at 700 °C exhibits only the orthorhombic phase (Figure 5C). Comparison of the product grown at 700 °C with a ceramic target (Figure 5D) does show, however, that thin film orthorhombic material grows with a preferential orientation on ⟨100⟩ $SrTiO_3$.

Several additional experiments were carried out to determine the influence of the substrate lattice on the growth of the meta-

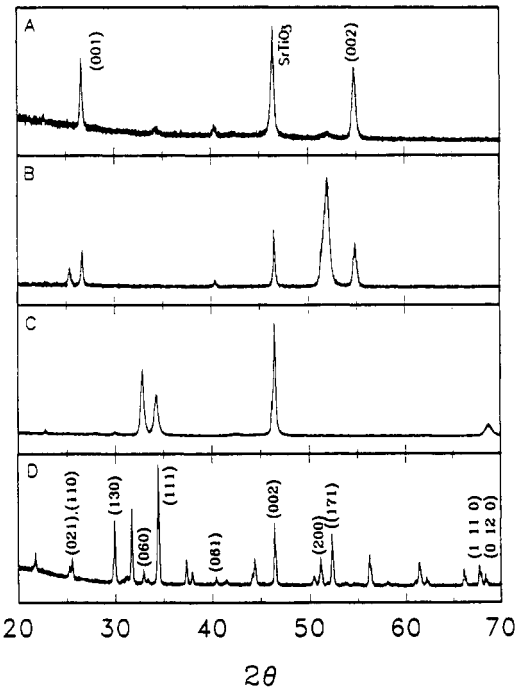

Figure 5. XRD diffraction patterns recorded on $SrCuO_2$ films grown on ⟨100⟩ $SrTiO_3$ by PLD at (A) 500 °C, (B) 600 °C, and (C) 700 °C. The XRD powder pattern for the orthorhombic $SrCuO_2$ target is shown in (D) for comparison.

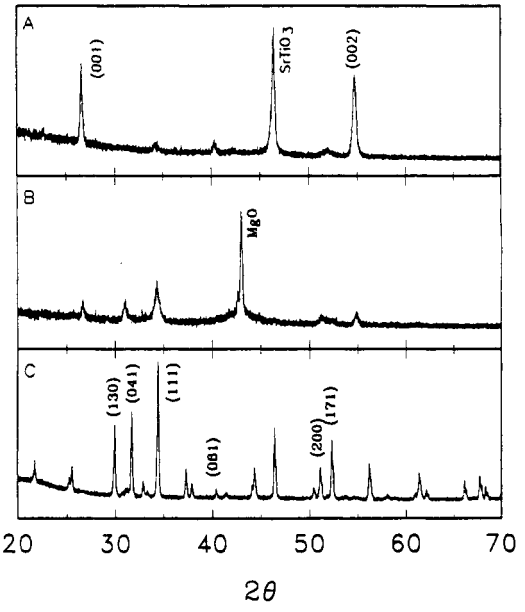

Figure 6. XRD diffraction patterns recorded on $SrCuO_2$ films grown on (A) ⟨100⟩ $SrTiO_3$ and (B) ⟨100⟩ MgO at 500 °C. The XRD pattern for orthorhombic $SrCuO_2$ is shown in (C) for comparison.

stable tetragonal phase. First, the growth of $SrCuO_2$ at 500 °C on ⟨100⟩ $SrTiO_3$ ($a = 3.905$ Å) was compared with growth at 500 °C on ⟨100⟩ MgO ($a = 4.20$ Å). XRD patterns of the materials grown on ⟨100⟩ MgO substrates exhibit a significant increase in the fraction of orthorhombic phase relative to films grown on ⟨100⟩ $SrTiO_3$ at the same temperature (Figure 6). Analyses of the peak intensities in Figure 6 indicate that only 30% of the material grown on ⟨100⟩ MgO is the tetragonal phase versus >90% of the product grown on ⟨100⟩ $SrTiO_3$. The importance of substrate lattice matching is further shown by ion channeling experiments. Comparison of the backscattering yields of ions obtained from random and aligned geometries on $Sr_{0.7}Ca_{0.3}CuO_2$ and $Sr_{0.16}Ca_{0.84}CuO_2$ materials grown at 500 °C on $SrTiO_3$ are shown in Figure 4. The minimum channeling yield for the

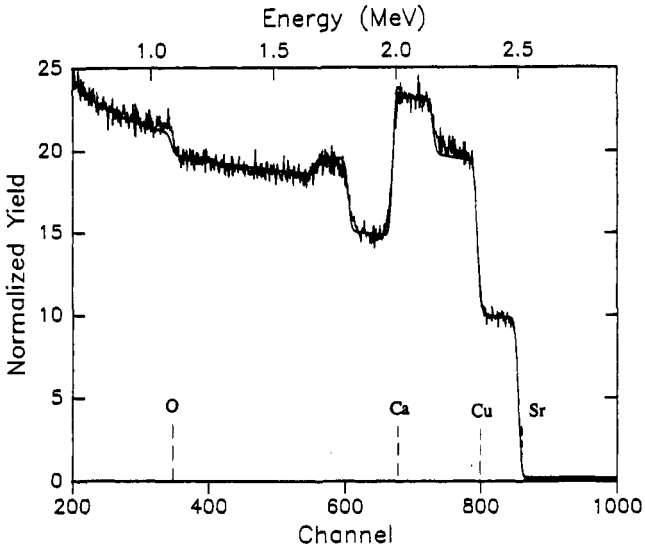

Figure 7. RBS data obtained on a nonstoichiometric $(Sr_{0.7}Ca_{0.3})_{0.9}CuO_2$ material prepared at 500 °C. The smooth solid line through the data corresponds to a fit for the composition $(Sr_{0.7}Ca_{0.3})_{0.9}Cu_{1.05}O_2$.

$Sr_{0.7}Ca_{0.3}CuO_2$ film is 5–6%. This low channeling yield indicates that the $Sr_{0.7}Ca_{0.3}CuO_2$ film grows epitaxially on $SrTiO_3$. The minimum channeling yield for the higher Ca^{2+} content material, 20%, is significantly larger. This larger channeling yield suggests that there are defects at the growth interface arising from mismatch of the $Sr_{0.7}Ca_{0.3}CuO_2$ *a*-axis with the $SrTiO_3$ lattice.

Synthesis and Characterization of Nonstoichiometric Materials. We have also investigated the synthesis of nonstoichiometric materials $(Sr_{1-x}Ca_x)_{1-\delta}CuO_2$, where δ corresponds to the average alkaline earth vacancy concentration in the films. A series of thin film $(Sr_{1-x}Ca_x)_{0.9}CuO_2$ materials with fixed nonstoichiometry were grown on ⟨100⟩ $SrTiO_3$ at 500 °C. XRD patterns recorded on the targets indicated that all of the $(Sr_{1-x}Ca_x)_{0.9}CuO_2$ materials prepared at high temperature were multiphase. In contrast, the diffraction patterns recorded on the thin films prepared by PLD can be indexed as the layered, tetragonal phase with the *c*-axis oriented perpendicular to the substrate surface. These data are similar to that shown in Figure 1 for the stoichiometric ($\delta = 0$) films. The metal-ion nonstoichiometry in the $(Sr_{1-x}Ca_x)_{0.9}CuO_2$ materials prepared by PLD was verified by RBS analyses. Typical data obtained on a film prepared using a $(Sr_{0.7}Ca_{0.3})_{0.9}CuO_2$ target are shown in Figure 7. The Sr/Ca/Cu composition of the film prepared at 500 °C was 0.63:0.27:1.05; hence, the 10% nonstoichiometry is preserved in the materials grown by PLD.

Physical Properties. The electrical and magnetic properties of the $(Sr_{1-x}Ca_x)_{1-\delta}CuO_2$ films have also been examined. The $\delta = 0$ materials all exhibit high resistivities. The magnetic properties of these near insulating compounds were not investigated. In contrast, significantly higher conductivities are observed for the $\delta = 0.1$ materials. It was also found that the electrical properties varied systematically as a function of x for this fixed nonstoichiometry. These results are summarized in Figure 8. The $x = 0.7$ and $x = 0.5$ materials exhibit activated transport below room temperature. The $x = 0.3$ and $x = 0$ samples show, however, weakly metallic behavior between 300 and 100 K. In addition, the $x = 0.7$, 0.5, and 0.3 samples exhibit sharp increases in resistivity at 250, 200, and 40 K, respectively (Figure 8A). The $x = 0$ $SrCuO_2$ material, however, exhibits a relatively sharp decrease in the resistivity with an onset at 20 K; a zero resistance state is achieved at 8 K in this material (Figure 8B). No magnetic transitions were observed between 4.2 and 100 K in low field (10 Oe) magnetization measurements.

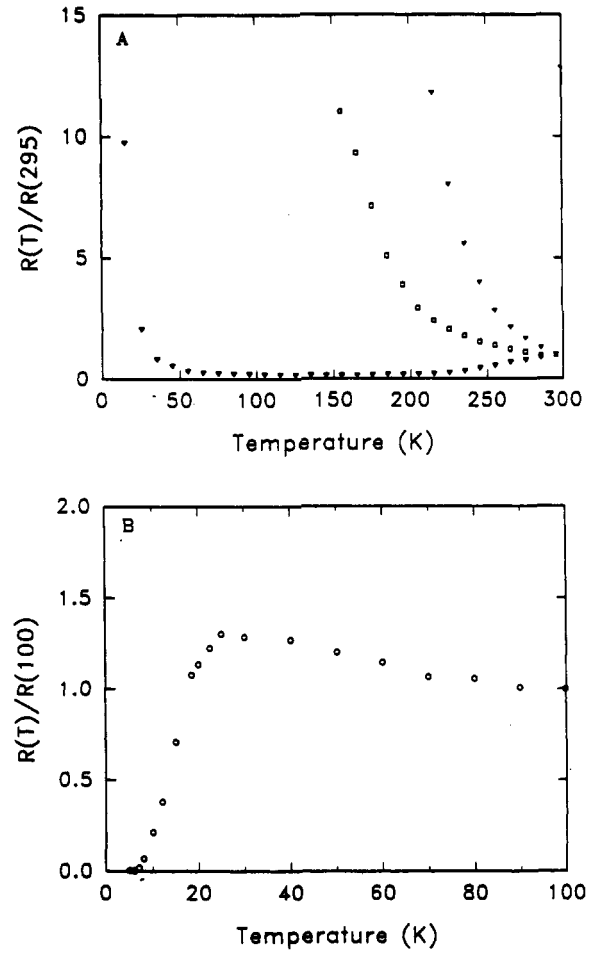

Figure 8. (A) Temperature dependent normalized resistivity data obtained on $(Sr_{0.3}Ca_{0.7})_{0.9}CuO_2$ (▼), $(Sr_{0.5}Ca_{0.5})_{0.9}CuO_2$ (□), and $(Sr_{0.7}Ca_{0.3})_{0.9}CuO_2$ (▽). (B) Normalized resistivity results obtained on a $Sr_{0.9}CuO_2$ sample.

Discussion

Growth of Layered $(Sr_{1-x}Ca_x)_{1-\delta}CuO_2$ Materials. The $Sr_{1-x}Ca_xCuO_2$ materials grown by PLD at 500 °C are structurally distinct from the target materials prepared by conventional high-temperature synthetic procedures. The high-temperature synthetic route used to prepare the $SrCuO_2$ targets yields an orthorhombic phase with $a = 3.57$ Å, $b = 16.34$ Å, and $c = 3.91$ Å (Figure 9A). The $Sr_{1-x}Ca_xCuO_2$ targets, $x > 0$, contain orthorhombic phase materials as well as other phases which we have not characterized. Notably, analysis of the materials prepared by PLD using X-ray diffraction, electron diffraction, and ion-channeling (Figure 1–4) shows that the structures of these materials correspond to a layered, tetragonal phase with the *c*-axis oriented perpendicular to the ⟨100⟩ $SrTiO_3$ substrate surface. This tetragonal layered phase is illustrated in Figure 9B. Simulations of the XRD and ED patterns based on *c*-axis oriented, tetragonal $MCuO_2$ are in excellent agreement with the experimental data and thus further support our structural assignment.

In general, the thin-film $Sr_{1-x}Ca_xCuO_2$ materials prepared by PLD at 500 °C are single phase (Figure 1). For the $x = 0$ material we also detect small impurity peaks at $2\theta = 34.4°$ and 40.3°; these peaks can be indexed as the (111) and (061) peaks of the orthorhombic phase. This impurity represents less than 5–10% of the product, and thus the major phase produced by PLD is tetragonal $SrCuO_2$. Although the $x > 0$ $Sr_{1-x}Ca_xCuO_2$ target materials are all multiphase, we find that $x > 0$ compounds prepared by PLD are all single phase with the layered, tetragonal structure. We find no impurity phases at the ≤5% detection limit set by background scattering in our experiments. In addition, we have found that "*x*" represents an accurate measure of the average metal stoichiometry in these thin film materials. The RBS data demonstrate that within experimental error the composition of the films are the same as that of the targets. Hence, PLD provides a ready method of growing a specific stoichiometry material even when the target is not single phase.

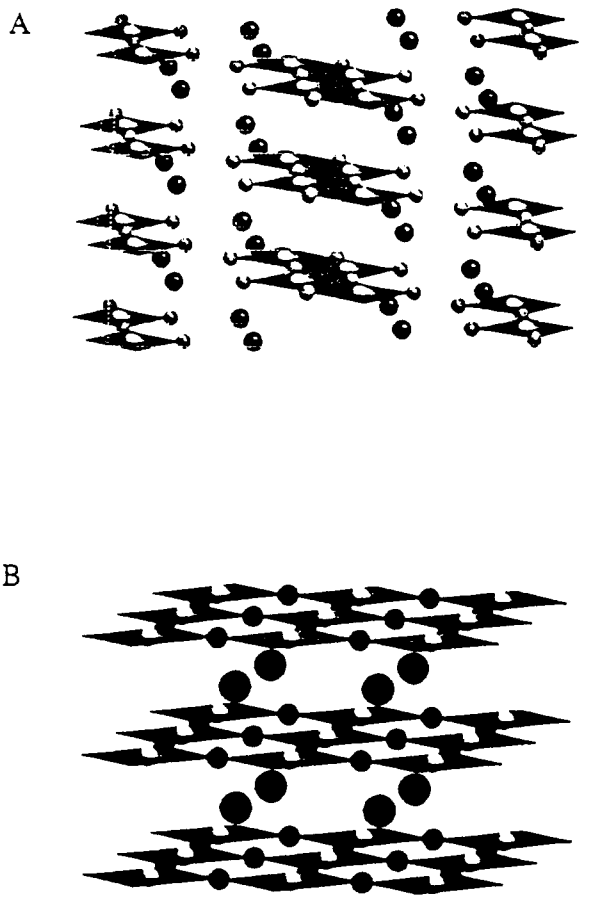

Figure 9. (A) View of the orthorhombic phase structure of the $MCuO_2$ materials illustrating the Cu–O double chains. (B) View of the tetragonal $MCuO_2$ structure highlighting the CuO_2 layers separated by alkaline earth cations.

We have also prepared a series of single-phase nonstoichiometric $(Sr_{1-x}Ca_x)_{0.9}CuO_2$ materials using low-temperature PLD. X-ray and electron diffraction data obtained on the nonstoichiometric materials shows that low-temperature growth from multiphase $(Sr_{1-x}Ca_x)_{0.9}CuO_2$ targets yields high-quality *c*-axis oriented tetragonal materials. Furthermore, RBS compositional analyses demonstrate that these materials contain 10% alkaline-earth vacancies. The RBS results are thus consistent with stoichiometric metal transfer from the target to the growth film. It is possible, that the thin film materials consist of domains of $(Sr_{1-x}Ca_x)CuO_2$ and CuO in a 10:1 ratio. However, we find no evidence for CuO or amorphous material in our ED measurements. In addition, it is likely that the Sr/Ca vacancies are distributed homogeneously in these layered tetragonal phase materials since the electrical properties change systematically with x in the $(Sr_{1-x}Ca_x)_{0.9}CuO_2$ materials (see below). Therefore, these results demonstrate that low-temperature PLD can be used to facilitate the synthesis of novel nonstoichiometric phases.

It is important to compare these new studies to past synthetic investigations. In general, it has not been possible to prepare the layered tetragonal phase of $MCuO_2$ using conventional high-temperature methods.[19,22,23] Synthesis of $SrCuO_2$ at ≈950 °C in air leads to the formation of a stable orthorhombic phase (Figure 9A).[19] The tetragonal phase, which is the parent structure of all of the copper oxide superconductors (Figure 9B), can only be obtained for the specific composition $Sr_{0.14}Ca_{0.86}CuO_2$ using conventional preparative methods.[22,23] Hence, it has not been possible to study systematically the substitutional chemistry and resulting physical properties of this phase. Several synthetic methods have been employed recently in efforts to provide general access to the tetragonal phase. First, ultrahigh pressure (20–65 kbar) and high-temperature (1000 °C) reaction have been used to prepare tetragonal $SrCuO_2$ and metal-substituted $SrCuO_2$.[24-26] Although these extreme conditions have been successful in obtaining the tetragonal phase, the small ceramic samples produced by the high-pressure reaction apparatus are not ideal for detailed physical studies. Furthermore, it has not been possible in previous high-pressure studies[24-26] to access systematically a range of compositions and stoichiometries as we have reported herein. PLD is also a useful technique for preparing this phase, but under much milder synthetic conditions (i.e., low temperature and pressure). Previous work in our group showed that $SrCuO_2$ could be prepared at low-temperature from a single target.[10] Kawai and co-workers were also able to obtain tetragonal $SrCuO_2$ via sequential deposition of Sr and Cu layers from two targets at 600 °C; however, the structures and compositions of these materials have not been well-characterized.[12] We believe that the single target approach used in our studies in advantageous since the metal ion stoichiometry can be accurately fixed during target preparation. Our present studies clearly demonstrate this point since we have been able to prepare, with excellent compositional control, a wide range of $(Sr_{1-x}Ca_x)_{1-\delta}CuO_2$ materials using single target PLD.

Mechanism of Growth. Since it has not been possible to prepare this wide range of materials previously by conventional methods, it is important to consider the factors affecting the growth of the tetragonal phase. We believe that the dominant factor is the low-temperature growth conditions possible with PLD. Low-temperature crystalline growth is possible in PLD since high-energy atomic and molecular species, which can readily diffuse at the growth interface, are generated in the laser ablation process.[9] In contrast, high temperatures are required to facilitate diffusion and reaction during conventional solid-state synthesis. Our temperature dependent growth studies (Figure 5) strongly support this proposal. These data show that as the temperature is increased the concentration of orthorhombic phase impurity increases, and by 700 °C the films are exclusively orthorhombic phase. These results strongly suggest that the metastable layered phase is trapped during low-temperature growth. It is possible that the product is either kinetically trapped or that the infinite layer phase represents the thermodynamically stable low-temperature phase. Interestingly, kinetic control is routinely utilized in complex molecular synthesis; however, high-temperature thermodynamics almost always dominate conventional solid-state synthesis. Hence, we believe that the ability to use low-temperature conditions in PLD synthesis is significant and should be broadly applicable to the preparation of new materials.

In addition, the substrate lattice plays a role in determining the orientation and growth of the tetragonal $(Sr_{1-x}Ca_x)_{1-\delta}CuO_2$ materials. We have shown that the thin films prepared at 500 °C on ⟨100⟩ $SrTiO_3$ grow with the *c*-axis of the tragonal $MCuO_2$ phase perpendicular to the substrate surface. Since the *a*-axis lattice constant of the $MCuO_2$ materials (a = 3.92 Å, M = Sr; a = 3.86 Å, M = $Sr_{0.14}Ca_{0.86}$) is similar to that of $SrTiO_3$ (a = 3.905 Å), we believe that lattice matching of the growing $MCuO_2$ phase to the ⟨100⟩ $SrTiO_3$ surface enforces a single orientation. This point is illustrated schematically in Figure 10. The layered tetragonal phase can be viewed as the $SrTiO_3$ structure missing all of the oxygen in the "SrO" planes. Assuming that ⟨100⟩ $SrTiO_3$ terminates with a SrO surface, then the first layer formed during PLD growth is CuO_2 with copper occupying the Ti position of $SrTiO_3$ (Figure 10). Alternatively, if the substrate surface is terminated in a TiO_2 layer, then it is expected that an oxygen deficient Sr layer would grow first followed by a CuO_2 layer.

(22) Siegrist, T.; Zahurak, S. M.; Murphy, D. W.; Roth, R. S. *Nature* **1988**, *334*, 231.
(23) Cava, R. J. *Nature* **1991**, *351*, 518.
(24) (a) Smith, M. G.; Manthiram, A.; Zhou, J.; Goodenough, J. B.; Markert, J. T. *Nature* **1991**, *351*, 549. (b) Er, G.; Miyamoto, Y.; Kanamura, F.; Kikkawa, S. *Physica C* **1991**, *181*, 206.
(25) (a) Takano, M.; Takeda, Y.; Okada, H.; Miyamoto, M.; Kusaka, T. *Physica C* **1989**, *159*, 375. (b) Takano, M.; Azuma, M.; Hiroi, Z.; Bando, Y. *Physica C* **1991**, *176*, 441.
(26) Azuma, M.; Hiroi, Z.; Takano, M.; Bando, Y.; Takeda, Y. *Nature* **1992**, *356*, 775.

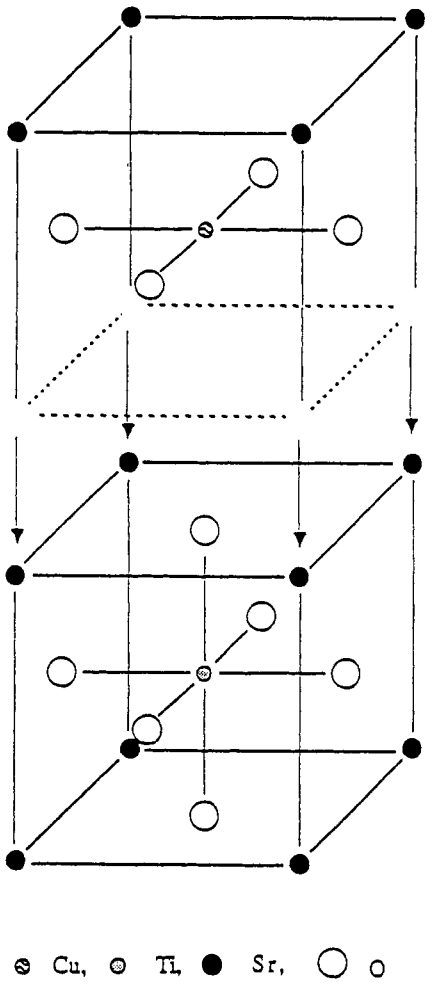

Figure 10. Schematic view of the growth of tetragonal $SrCuO_2$ on a ⟨100⟩ $SrTiO_3$ surface that terminates in a Sr–O layer.

Several pieces of additional experimental evidence support our proposal of lattice-matched or epitaxial growth. First, the high-energy channeling yield for $Sr_{0.7}Ca_{0.3}CuO_2$ (a = 3.90 Å), 6%, is significantly lower than the 20% yield observed for $Sr_{0.14}Ca_{0.86}CuO_2$ (a = 3.86 Å). The 6% yield indicates excellent epitaxial growth and is consistent with the very good lattice match to the $SrTiO_3$ substrate. In addition, this low channeling yield shows that the $Sr_{0.7}Ca_{0.3}CuO_2$ product is well-oriented and highly crystalline. The higher channeling yield observed for the $Sr_{0.14}Ca_{0.86}CuO_2$ film is expected since this material has a poorer lattice match with the substrate. Furthermore, we have shown that PLD growth of $SrCuO_2$ on ⟨100⟩ MgO (a = 4.20 Å) leads to a greater concentration of orthorhombic impurity phase than in materials grown under identical conditions on $SrTiO_3$. These results also support our proposal since the lattice mismatch is significantly larger on MgO (7%) than $SrTiO_3$ (0.4%).

Physical Properties. Lastly, we consider the variation in physical properties of this series of $(Sr_{1-x}Ca_x)_{1-\delta}CuO_2$ compounds. We believe that an important characteristic of materials prepared by PLD is the high degree of orientation and crystallinity that they exhibit; that is, these compounds are single crystal-like and are thus well suited for many physical studies. Resistivity measurements have shown that all of the stoichiometric $Sr_{1-x}Ca_xCuO_2$ materials are insulating. This insulating behavior is not unexpected since extensive studies of the copper oxide superconductors have shown that the undoped Cu(II) state of these materials is an antiferromagnetic insulating state.[27] The near insulating character of the $Sr_{1-x}Ca_xCuO_2$ materials indicates, however, that these compounds do not have a high concentration of defects since nonstoichiometry will lead to metallic behavior.

(27) Batlogg, B. *Physics Today* **1991**, *44*, 44.

The resistivity data obtained on the nonstoichiometric $(Sr_{1-x}Ca_x)_{0.9}CuO_2$ materials differ significantly from the results obtained on the stoichiometric compounds (Figure 8). The x = 0.7 and x = 0.5 materials exhibit activated transport below 300 K, while the x = 0.3 and x = 0 compounds are weakly metallic between 300 and 100 K. In addition, the x = 0.7, 0.5, and 0.3 materials exhibit sharp increases in resistivity (i.e., a transition to a highly insulating state) at 250, 200, and 40 K, respectively. The x = 0 compounds show a transition to a zero resistance state at ≈20 K, although magnetic susceptibility measurements indicate that these materials are not bulk superconductors. The results thus indicate that the $(Sr_{1-x}Ca_x)_{0.9}CuO_2$ materials become increasingly metallic and possibly superconducting as x approaches zero. These data may seem somewhat surprising since the metal nonstoichiometry is the same in the four materials, and thus to a first approximation the carrier concentration should be constant. However, it is also important to consider the coordination of Cu since alkaline earth vacancies formally create holes in the copper oxide layers. In the ideal $(Sr_{1-x}Ca_x)_{0.9}CuO_2$ structure Cu remains four-coordinate (Figure 9B). However, in all of the known hole-doped copper oxide superconductors Cu is either five- or six-coordinate.[28] We thus speculate that five-coordinate Cu, which is produced by axial oxygen coordination, is essential for enhanced conductivity in these materials. Since axial oxygens will fit more readily in $(Sr_{1-x}Ca_x)_{0.9}CuO_2$ materials that have a larger c-axis (i.e., smaller value of x),[29] the above hypothesis is consistent with the observed trend in the resistivity results (Figure 8). In the future it will be important to test these ideas by investigating nonstoichiometric materials deposited in different oxygen pressures.

Lastly, it is interesting to compare these results to other recent studies of nonstoichiometric $M_{1-\delta}CuO_2$ materials.[12b,26] Recent ultrahigh pressure studies of $(Sr_{0.7}Ca_{0.3})_{0.9}CuO_2$ materials have provided evidence for an onset to superconductivity at 110 K.[26] Our PLD results are similar in that resistivity measurements indicate $Sr_{0.9}CuO_2$ is a superconductor, although we do not observe evidence for superconductivity in $(Sr_{0.7}Ca_{0.3})_{0.9}CuO_2$. It is possible that these differences are due to small variations in the oxygen content.[30] In addition, Kawai and co-workers have reported superconductivity in $Sr_{1-x}Ca_xCuO_2$ materials prepared by multitarget PLD.[12b] Our PLD results contrast this work since we find insulating behavior in materials that have a 1:1 alkaline earth/copper ratio. We believe that a likely explanation for the observed differences is that the films prepared from independent Sr/Ca and Cu targets are nonstoichiometric, although additional studies will be needed to prove this point.

Conclusions

In summary, we have used PLD to study the synthesis of a series of $(Sr_{1-x}Ca_x)_{1-\delta}CuO_2$ materials. In contrast to conventional high-temperature methodology, we have shown that low-temperature PLD synthesis leads to the formation of single phase metastable materials that have a layered, tetragonal structure and that the tetragonal structure is obtained over a wide range of stoichiometries (x and δ). Mechanistic studies have demonstrated several important points, including the following: (i) that low-temperature growth, which is accessible with PLD, traps the metastable tetragonal phase of the $(Sr_{1-x}Ca_x)_{1-\delta}CuO_2$ materials; (ii) that substrate–product lattice matching helps to crystallographically orient and stabilize the tetragonal phase; and (iii) that there is stoichiometric metal transfer from the target to the growing film even when the target is not single phase. We believe these mechanistic results are especially significant since they show that it is possible to utilize kinetic control and other factors to prepare novel materials. In addition, the $(Sr_{1-x}Ca_x)_{1-\delta}CuO_2$ materials prepared in this study represent an ideal model system

(28) Sleight, A. W. *Science* **1988**, *242*, 1519.

(29) The c-axis increases as the value of x decreases and thus creates a larger average vacancy volume.

(30) It is not possible to measure accurately the oxygen content using RBS spectroscopy. We believe, therefore, that it will be important in the future to carry out systematic studies of materials prepared in different oxygen environments.

for the copper oxide superconductors. Our preliminary physical studies demonstrate that the electrical properties change systematically with variations in x and δ, and, furthermore, these data provide evidence for superconductivity in $Sr_{0.9}CuO_2$. We believe that continued efforts using PLD to prepare crystalline $MCuO_2$ materials containing different (i) metals, (ii) metal stoichiometries, and (iii) oxygen stoichiometries will lead to new superconducting phases and to an improved understanding of superconductivity in the copper oxide materials.

Acknowledgment. Use of the Harvard NSF-MRL facilities is gratefully acknowledged. C.M.L. also thanks the David and Lucile Packard and National Science Foundations for partial support of this work.

Quantitative Expression of Dynamic Kinetic Resolution of Chirally Labile Enantiomers: Stereoselective Hydrogenation of 2-Substituted 3-Oxo Carboxylic Esters Catalyzed by BINAP-Ruthenium(II) Complexes

M. Kitamura, M. Tokunaga, and R. Noyori*

Contribution from the Department of Chemistry, Nagoya University, Chikusa, Nagoya 464-01, Japan. *Received August 10, 1992*

Abstract: Hydrogenation of chirally unstable 2-substituted 3-oxo carboxylic esters gives a mixture of four stereoisomeric hydroxy esters. Use of BINAP-Ru(II) complex catalysts allows selective production of one stereoisomer among four possible isomers. The stereoselectivity obtained by the dynamic kinetic resolution depends on facile in situ racemization of the substrates, efficient chirality recognition ability of the catalysts, and the structures of the ketonic substrate. The factors controlling the efficiency of the stereoselective hydrogenation are experimentally determined by reaction of racemic oxo esters using enantiomerically pure and racemic BINAP complexes. Quantitative expression of the dynamic kinetic resolution has been made by defining the product partition coefficients (w, x, y, and z), the relative reactivities of the enantiomeric substrates (k_{fast}/k_{slow}), and the relative ease with which stereoinversion and hydrogenation take place (k_{inv}/k_{fast}). The validity of the equations has been demonstrated by the graphical exhibition of the enantioselectivity and diastereoselectivity as a function of conversion of the substrates.

Under certain chiral circumstances, substrate enantiomers S_R and S_S react at different rates, k_R and k_S, yielding enantiomeric products P_R and P_S as illustrated in Scheme I. This principle allows chemical or biological kinetic resolution of racemic compounds. As studied extensively by Kagan, Sharpless, Sih, and others,[1] the k_R/k_S ratio of eq 1 is correlated to the extent of

$$\frac{k_R}{k_S} = \frac{\ln (1 - \text{convn})(1 - \text{ee}_S)}{\ln (1 - \text{convn})(1 + \text{ee}_S)} = \frac{\ln [1 - \text{convn}(1 + \text{ee}_P)]}{\ln [1 - \text{convn}(1 - \text{ee}_P)]} \quad (1)$$

substrate conversion and the enantiomeric excess of the recovered substrate and product, ee_S and ee_P, respectively. This value has been utilized for assessing the efficiency of the resolution.[2] Such ordinary kinetic resolution, though very useful, suffers from the inherent disadvantage that the maximum yield of one enantiomer is 50% and, furthermore, that ee's of the product and recovered substrate are profoundly influenced by the extent of conversion. On the other hand, racemic compounds possessing a chirally labile stereogenic center allowing its in situ racemization during reaction can, in principle, be converted in 100% yield to enantiomerically pure products regardless of the extent of substrate conversion. This paper further elaborates on the dynamic kinetic resolution of enantiomers outlined in Scheme II. This reaction system is characterized not only by the presence of the substrate stereoinversion, $S_R \rightleftarrows S_S$, but also by formation of diastereomeric products, where both enantioselection and diastereoselection are exhibited.[3] Thus, under appropriate conditions, this kinetic resolution method can convert a racemic compound to one stereoisomer among many. In Scheme II the competitive reactions are closely interrelated, in contrast to the conventional kinetic resolution of Scheme I where the two pathways are independent of one another. Although the

Scheme I

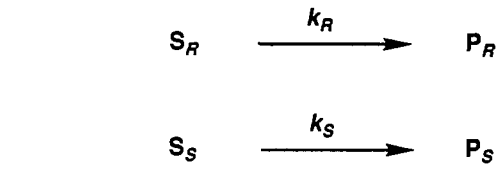

Scheme II

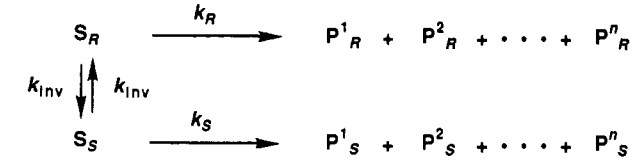

(1) Reviews: (a) Kagan, H. B.; Fiaud, J. C. *Top. Stereochem.* **1988**, *18*, 249. (b) El-Baba, S.; Nuzillard, J. M.; Poulin, J. C.; Kagan, H. B. *Tetrahedron* **1986**, *42*, 3851. (c) Chen, C.-S.; Sih, C. J. *Angew. Chem., Int. Ed. Engl.* **1989**, *28*, 695. (d) Finn, M. G.; Sharpless, K. B. In *Asymmetric Synthesis*: Morrison, J. D., Ed.; Academic Press: New York, 1985; p 247.

(2) For earlier studies on the relation between ee of substrate or product and conversion, see: Bredig, G.; Fajans, K. *Ber. Dtsch. Chem. Ges.* **1908**, *41*, 752. Fajans, K. *Z. Phys. Chem.* **1910**, *73*, 25. Kuhn, W.; Knopf, E. *Z. Z. Phys. Chem. Abstr., B* **1930**, *7*, 292. Newman, P.; Rutkin, P.; Mislow, K. *J. Am. Chem. Soc.* **1958**, *80*, 465. Balavoine, G.; Moradpour, A.; Kagan, H. B. *J. Am. Chem. Soc.* **1974**, *96*, 5152. Danishefsky, S.; Cain, P. *J. Am. Chem. Soc.* **1976**, *98*, 4975. Meurling, L.; Bergson, G.; Obenius, U. *Chem. Scr.* **1976**, *9*, 9. Izumi, Y.; Tai, A. In *Stereo-Differentiating Reactions*; Academic Press: New York, 1977; p 119.

(3) Kinetic resolution combined with the creation of an asymmetric center: Guettē, J.-P.; Horeau, A. *Bull. Soc. Chim. Fr.* **1967**, 1747. El-Baba, S.; Poulin, J.-C.; Kagan, H. B. *Tetrahedron* **1984**, *40*, 4275.

0002-7863/93/1515-144$04.00/0